Biochemistry

 Volume 37, Number 33 August 18, 1998

Accelerated Publications

Phosphorylation Stabilizes the Active Conformation of Rhodopsin†

Scott K. Gibson, John H. Parkes, and Paul A. Liebman*

Department of Biochemistry and Biophysics, University of Pennsylvania Medical Center, Philadelphia, Pennsylvania 19104-6059

Received April 24, 1998

ABSTRACT: Deactivation of many G protein coupled receptors (GPCRs) is now known to require phosphorylation of the activated receptor. The first such GPCR so analyzed was rhodopsin, which upon light activation forms an intramolecular equilibrium between the two conformers, metarhodopsin I and II (MI and MII). In this study, we find surprisingly that rhodopsin phosphorylation increases rather than diminishes the formation of MII, the conformation that activates G protein. The MI−MII equilibrium constant was progressively shifted toward MII as the experimental phosphorylation stoichiometry was increased from 0 to 6.4 phosphates per rhodopsin. Increasing phosphorylation both increased MII's formation rate (k_1) and decreased its rate of loss (k_{-1}). The direct effect of cytoplasmic surface phosphorylation on intramolecular conformer equilibria observed here may be important to functional state modulation of other membrane proteins.

G protein coupled receptors (GPCRs)[1] are thought to exist in several intramolecular equilibrium configurations, one of which is selected by agonist binding: this state activates G proteins. The activity and lifetime of activated receptors are regulated by receptor phosphorylation (*1*−*4*), a reaction catalyzed by G protein coupled receptor kinases (GRKs) (*5*−*7*).

Rhodopsin is perhaps the best-understood GPCR. Its active site contains the chromophore, 11-*cis*-retinal, which acts as resting state receptor antagonist (*8*, *9*). Absorbed light isomerizes 11-*cis*- to *all*-*trans*-retinal, the agonist for rhodopsin activation. The receptor then relaxes into a long-lived pH and temperature-dependent equilibrium between the two spectroscopic species, metarhodopsin I and II (MI and MII). MII (λ_{max} 387 nm), the dominant species present at body temperature, is the protein conformation responsible for activation of the retinal G protein, transducin (*10*−*12*). At lower temperatures or higher pH, the equilibrium is shifted toward MI (λ_{max} 480 nm), a form that does not activate G protein. The remarkable change in light absorption properties accompanying formation of MI and MII provides a natural spectroscopic probe that has been used to monitor the distribution between these states of the receptor during their formation and subsequent dissipation.

Activated rhodopsin is phosphorylated on C-terminal serines and threonines by rhodopsin kinase (GRK1) (*13*−*15*). Phosphorylation is essential to rapid quenching of the visual transduction cascade (*1*, *2*, *5*). High phosphorylation stoichiometries, up to nine phosphates per rhodopsin found in vitro (*16*), can directly terminate signaling (*17*) or can be augmented by arrestin binding at lower ratios (*18*). Multiple

† Supported by NIH Grants EY00012, EY01583, and EY07035.

* Address correspondence to this author. Telephone: 215-898-6917. FAX: 215-898-4217. Email: liebmanp@mail.med.upenn.edu.

[1] Abbreviations: GPCR, G protein coupled receptor; GRK, G protein receptor kinase; λ_{max}, maximum absorbance wavelength; MI, metarhodopsin I; MII, metarhodopsin II; MIII, metarhodopsin III; RDM, rod disk membrane; EDTA, ethylenediaminetetraacetic acid; NADPH, β-nicotinamide adenine dinucleotide phosphate, reduced form; DTT, dithiothreitol; OD, optical density; POPC, 1-palmitoyl-2-oleoyl-*sn*-glycero-3 phosphocholine; PC, phosphatidylcholine; PS, phosphatidylserine.

S0006-2960(98)00933-7 CCC: $15.00
Published on Web 07/29/1998

phosphorylation is a candidate mechanism for explaining graded turnoff of activated receptors (*19*).

In this report, we show that rhodopsin phosphorylation also modulates the MI−MII equilibrium constant itself, unexpectedly increasing the amount of MII formed with increasing receptor phosphorylation. Companion kinetic analysis showed phosphorylation to both increase the rate of MII formation (k_1) and decrease the back rate from MII to MI (k_{-1}). This effect might be important in accelerating multiple (cooperative) phosphorylation by enriching MII, favoring early binding of arrestin to phosphorylated MII, or enhancing loss of activity through more MIII formation at higher bleach levels.

EXPERIMENTAL PROCEDURES

Preparation of Rod Disk Membranes. Retinas were dissected under infrared light from bovine eyes freshly obtained from a local slaughterhouse (MOPAC; Souderton, PA). Rod disk membranes (RDM) were purified by sucrose density gradient centrifugation as previously described (*20*). Rhodopsin concentration was determined from the absorption spectrum of each RDM sample using the Dartnall correction for light scattering (*21*).[2]

Preparation of Phosphorylated Rhodopsin. Rhodopsin was phosphorylated according to the method of Wilden and Kühn (*16*). Briefly, RDM samples containing 12.5 μM rhodopsin, 3 mM ATP, 1 mM $MgCl_2$, 1 mM DTT, and 100 mM NaH_2PO_4, pH 7.4, were phosphorylated in 12 × 75 mm optically transparent polystyrene tubes (Falcon; Lincoln Park, NJ) held in a 30 °C water bath. Phosphorylation was initiated by exposure to a 60 W tungsten lamp, placed 20 cm from the tubes. Reaction tubes were frequently agitated to ensure uniform illumination. Control, unphosphorylated samples were treated identically except for the absence of ATP.

One identical RDM phosphorylation tube containing [γ-^{32}P]ATP at 2.7 μCi/μmol (Dupont NEN; Boston, MA) was used to monitor phosphate incorporation progress and stoichiometry. At selected times, 100 μL aliquots were removed from it and transferred to 700 μL of ice-cold quenching solution (100 mM, pH 7.4, NaH_2PO_4, 20 mM EDTA). RDM were then pelleted by centrifugation, washed twice with 700 μL of 100 mM NaH_2PO_4, pH 7.4, and either counted in a Quick-Count benchtop radioisotope counter (Bioscan; Washington, DC) or solubilized in Ecolume Scintillation Cocktail (ICN; Costa Mesa, CA) and later counted in a liquid scintillation counter (Intertechnique; Fairfield, NJ). Nonradioactive reaction samples were stopped similarly and used in the spectroscopic experiments after pigment regeneration described below. Phosphorylation stoichiometry was calculated by dividing the moles of phosphate incorporated by the moles of rhodopsin. Phosphorylation stoichiometry was varied by increasing the incubation time from 0 to 160 min.

Bleached phosphorylated and unphosphorylated control samples were regenerated on ice with a 3-fold excess of 11-*cis*-retinal (a generous gift from R. K. Crouch and the National Eye Institute) for at least 12 h of dark incubation followed by a further 1 h incubation at 30 °C to ensure completion. Before determination of the regenerated rhodopsin concentration, the excess 11-*cis*-retinal (λ_{max} 380 nm) was reduced to 11-*cis*-retinol (λ_{max} ~320 nm) by incubating with NADPH in 10-fold excess over the starting rhodopsin concentration in the presence of native retinal reductase for 1 h at 30 °C. Regeneration was confirmed to be 100 ± 5% complete by absorption spectroscopy.

The phosphorylated, regenerated RDM were then hypotonically stripped to remove peripheral proteins (*5*). The final pellet was suspended in 10 mM KH_2PO_4, pH 7.0, 0.1 mM EDTA, 1 mM DTT, and 100 mM KCl to form a stock of RDM at approximately 250 μM rhodopsin. Stocks were purged with argon and held on ice in dark storage containers. Aliquots were diluted from the stock concentration for spectroscopy.

Incremental Bleach Methodology. An incremental rhodopsin bleaching method (*22*, *23*) was used to determine the MI−MII equilibrium constant and the fraction of rhodopsin bleached in RDM suspensions at several phosphorylation levels. Briefly, 19 serial light flashes of equal intensity were used to bleach 3−4% of the remaining rhodopsin per flash at 50 s intervals. MII formation was monitored by kinetically measuring the increase in absorbance at 390 nm while subtracting the accompanying light scattering change (*24*) at the nearby MI−MII isosbestic wavelength (426 nm). At pH 7.0, this resulted in an upward staircase of absorbance increments, individual steps diminishing exponentially in amplitude, analogous to radioactive decay, as the remaining unbleached rhodopsin was depleted with each flash (Figure 1).

All spectral data were acquired using an SLM/Aminco DW2000 dual-wavelength spectrophotometer (Urbana, IL) equipped with an EG&G Electrooptics (Salem, MA) xenon flash unit (FX-199 tube, PS-302 power supply set at 500 V, with a 7 μF external capacitor) and a thermally jacketed cuvette holder connected to a constant temperature water circulator. Optical filters were used to limit the bleaching flash to wavelengths between 420 and 680 nm. Experimental samples contained about 10 μM rhodopsin (assayed exactly for each experimental run) in 10 mM KH_2PO_4, pH 7.00, 100 mM KCl, and 0.01 mM EDTA. Substitution of MOPS [3-(*N*-morpholino)propanesulfonic acid] for phosphate buffer did not alter the results. The measurements were made at 0.5 °C to minimize slow conversion of MII into MIII during the course of an experiment (see below).

Determination of MI−MII Equilibrium Constant and Fraction Bleached. The reactions studied are depicted in Scheme 1:

Scheme 1

$$\mathrm{Rh} \xrightarrow{\text{light}} \mathrm{MI} \underset{k_{-1}}{\overset{k_1}{\rightleftharpoons}} \mathrm{MII}$$

The MI and MII concentrations that occur after each flash and their K_{eq} value can be determined as follows: if $[Rh]_0$ is the initial rhodopsin concentration, f the fraction of rhodopsin bleached per flash, [Rh*] the concentration of bleached rhodopsin, and re a correction for photoregeneration, the fraction of rhodopsin activated by the nth flash is (*23*)

[2] $[Rh] = [1.10(OD_{500}) - 0.77(OD_{600}) - 0.33(OD_{400})]/40000\ cm^{-1}\ M^{-1}$.

$$[\mathrm{Rh}^*]_n = f[1 - (f)(re + 1)]^{(n-1)} \times [\mathrm{Rh}]_0 \quad (1)$$

When MI and MII are the only photoproducts formed, Rh* = MI + MII, and at equilibrium:

$$K_{eq} = \frac{[\mathrm{MII}]}{[\mathrm{MI}]} = \frac{k_1}{k_{-1}} \quad (2)$$

$$[\mathrm{MI}] = \frac{1}{1 + K_{eq}} \times [\mathrm{Rh}^*] \quad (3)$$

$$[\mathrm{MII}] = \frac{K_{eq}}{1 + K_{eq}} \times [\mathrm{Rh}^*] \quad (4)$$

The change in optical density (ΔOD) per flash is

$$\Delta\mathrm{OD} = \Delta[\mathrm{MI}] \times \Delta\epsilon_{(\mathrm{Rh}\rightarrow\mathrm{MI})} + \Delta[\mathrm{MII}] \times \Delta\epsilon_{(\mathrm{Rh}\rightarrow\mathrm{MII})} \quad (5)$$

where Δ[MI] and Δ[MII] are the concentrations of MI and MII formed per flash and $\Delta\epsilon_{(\mathrm{Rh}\rightarrow\mathrm{MI})}$ ($-7200\ \mathrm{M^{-1}\ cm^{-1}}$) and $\Delta\epsilon_{(\mathrm{Rh}\rightarrow\mathrm{MII})}$ ($34\,800\ \mathrm{M^{-1}\ cm^{-1}}$) are the Rh→MI and Rh→MII differential extinction coefficients at 390/426 nm.

Under our conditions, the MI−MII equilibrium is established within a few seconds after a bleaching light flash. Improved data precision in evaluating this equilibrium was obtained if the change in absorbance (ΔOD) was determined by averaging data over the last 40 s following each flash, and subtracting the similar average obtained from the previous flash. These equilibrium values were then fitted using the above equations in a Simplex algorithm which determined the least-squares best-fitting MI−MII equilibrium constant (K_{eq}) and fraction bleached (f) per flash for a single incremental bleach series (Parkes and Liebman, personal communication).

Recent studies have identified additional 380 nm intermediates that form faster than MII, which suggests that the classical model of MII formation proposed by Matthews et al. (*25*) (Scheme 1) may be incomplete. These intermediates, however, were only found in detergent extracts (*26*) or at temperatures above 25 °C (*27*); therefore, the classical model appears correct for our conditions.

Refinements. Data resulting from the first two flashes were not used in the fit because small amounts of G_t that remain in hypotonically stripped RDM could bind to and stabilize MII (*10*), increasing the apparent equilibrium constants for MII formation. There appeared to be little or no MII stabilization by residual G_t after the second flash.

At higher phosphorylation levels, the kinetic records exhibited a downward slope that increased with the amount bleached and with the degree of phosphorylation, presumably due to an increasing rate of formation of MIII (λ_{max} ~460 nm) from MII. Failure to correct for this OD loss would result in an underestimation of the MI−MII equilibrium constant. The rate of MIII formation should be proportional to the amount of MII present, which should steadily increase with successive bleaches; therefore, the magnitudes of the slopes for each individual bleach series were fit to a single exponential, and the smoothed values of the negative slopes were added back to correct the kinetic data.

Analysis of Kinetic Data. We obtained a single kinetic record for MII formation of substantially improved signal-to-noise ratio by averaging the last 17 absorbance responses in each 19 flash series. The resulting record was well fitted by a single exponential rate constant, k_{obs}. The forward (k_1) and reverse (k_{-1}) rate constants contributing to k_{obs} were then determined as previously described (*22*).

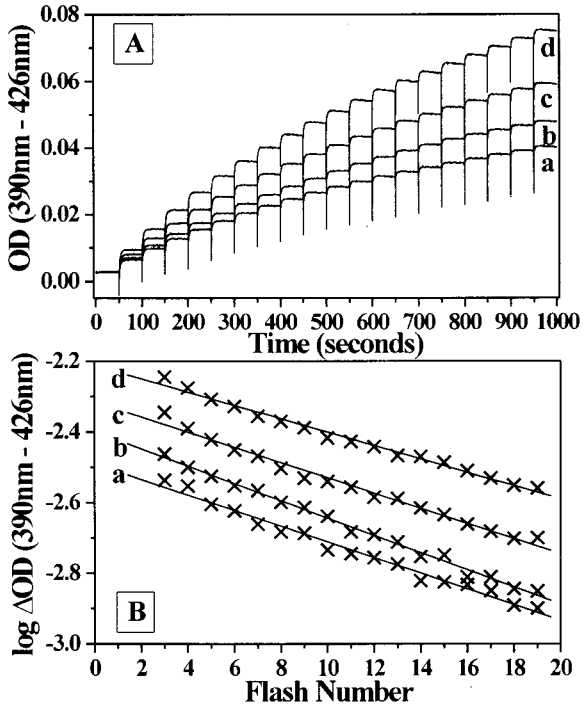

FIGURE 1: Effect of serial bleaches of constant intensity on regenerated rhodopsin samples with phosphorylation stoichiometries of (a) 0.0, (b) 1.3, (c) 3.0, and (d) 5.3 phosphates per rhodopsin. (A) MII formation at 0.5 °C was measured at 390 nm minus 426 nm. All data have been normalized to 10 μM rhodopsin. The downward spikes are due to flash artifact and MI formation. (B) The increments in OD in panel A, corrected for MIII formation, are plotted on a log scale. The linearity of the data shows that the fraction of remaining rhodopsin bleached is constant; that the fits are nearly parallel shows that the fraction bleached is unchanged at different phosphorylation levels.

RESULTS

The effect of phosphorylation on MII formation was examined by serially bleaching rhodopsin samples with different average phosphorylation stoichiometries as described under Experimental Procedures. Figure 1 illustrates that phosphorylated rhodopsin undergoes a larger change in OD than does unphosphorylated rhodopsin for the same intensity flash. Higher phosphorylation levels yield progressively larger increases in OD. An increasing change in OD with phosphorylation might be due either to an increasing fraction bleached or to increased MII formed per constant bleach (K_{eq} increase).

Our Simplex modeling analysis showed, however, that phosphorylation did not alter the fraction bleached. This is demonstrated intuitively in Figure 1B where the slopes were invariant with phosphorylation stoichiometry. Instead, K_{eq} was found to steadily increase with increasing phosphorylation (Figure 2). K_{eq} values for control, unphosphorylated RDM ranged from 0.52 to 0.59; these values approximately tripled to a value of 1.5 at 6.4 phosphates per rhodopsin (Figure 2).

The kinetics of the responses to individual bleaching flashes suggested that the rate of MII formation was also

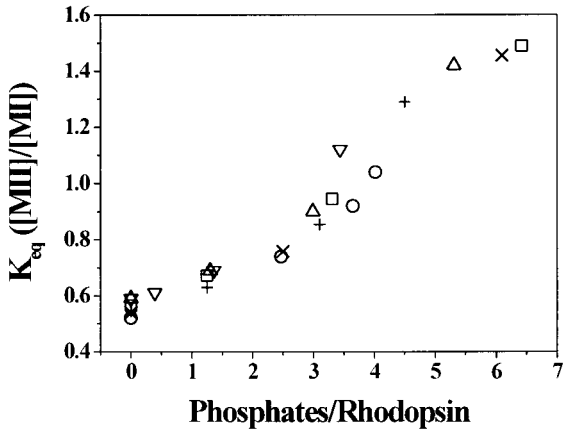

FIGURE 2: K_{eq} values determined by analysis of equilibrium data like that in Figure 1B for phosphorylation stoichiometries between 0 and 6.4. Each symbol type is a different RDM preparation.

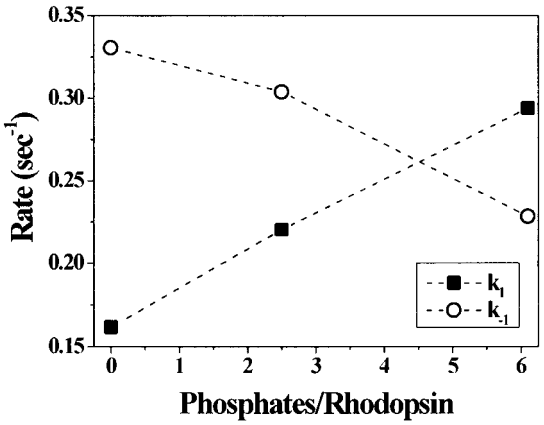

FIGURE 3: Rate constants for MI−MII conversion were determined by fitting an averaged flash response to a single exponential (k_{obs}). The individual rate constants (k_1 and k_{-1}) were determined from k_{obs} as discussed under Experimental Procedures. The negative slopes resulting from MIII formation were corrected, and data perturbed by G protein binding were omitted.

faster with increasing receptor phosphorylation. Comparison of the exponential time constants showed the MII formation rate constant, k_1, to increase from 0.16 s^{-1} for unphosphorylated rhodopsin to 0.29 s^{-1} at 6.1 phosphates per rhodopsin. The reverse rate constant, k_{-1}, decreased from 0.33 s^{-1} for the control (no phosphates) to 0.23 s^{-1} at 6.1 phosphates per rhodopsin (Figure 3).

K_{eq} could be calculated as a ratio of the rate constants obtained from the kinetic analysis (eq 2). The good agreement between values of K_{eq} determined by these independent kinetic and equilibrium methods (Figure 4) provides additional confidence in the accuracy of the values determined for K_{eq}, k_1, and k_{-1} under each of the phosphorylation conditions.

In the absence of phosphorylation, however, MIII formation was negligible at the low temperatures and neutral pH of our experiments. With phosphorylation, however, this was no longer true (downward slopes in Figure 1A). This is at least partly caused by the increase in K_{eq}, which, at six phosphates per rhodopsin, nearly doubles the amount of MII formed. This must increase the rate of MIII formation by mass action.

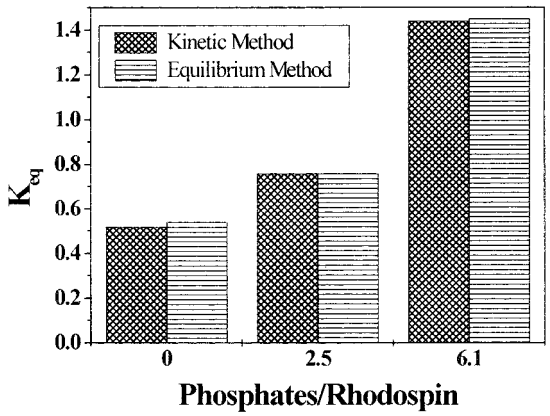

FIGURE 4: Comparison of the values of K_{eq} calculated as the ratio of kinetic rate constants with the values calculated from least-squares fitting of the equilibrium data to eqs 1−5 under Experimental Procedures.

DISCUSSION

The discovery that ATP rapidly quenches activation of the visual signal transduction cascade via phosphorylation of rhodopsin (*1*, *2*) by rhodopsin kinase (*5*, *28*) was the antecedent to subsequent studies implicating GPCR phosphorylation by GRKs as a paradigm for the regulation of all GPCR signaling (*7*). Phosphorylation appears to provide a new receptor configuration that can directly block activity (*17*) or can bind the blocking protein, arrestin (*29*).

The shift of the MI−MII equilibrium toward MII with increasing receptor phosphorylation reported here is an additional effect of phosphorylation that has escaped previous notice. This occurs through an increase in the forward rate constant (k_1) for MII formation with increasing receptor phosphorylation while the back rate constant (k_{-1}) decreases, both effects contributing to the increase in K_{eq}.

The equilibrium between MI and MII is known to be affected by a number of external variables such as pH and temperature (*22*, *25*), pressure (*30*, *31*) and lipid environment (*32*, *33*). The exact mechanism causing MII to be stabilized by phosphorylation is not yet known. We found the absorption spectrum of rhodopsin was unchanged by phosphorylation, suggesting that phosphorylation-induced conformational changes are not large or do not affect receptor core structure. Local conformational changes caused by phosphorylation might not alter the chromophore binding pocket but could conceivably alter K_{eq} through more peripheral actions.

A previous report by Mitchell et al. (*34*) concluded that rhodopsin phosphorylation does not alter K_{eq}. These authors studied phosphorylated rhodopsin reconstituted into POPC lipid vesicles. By contrast, our measurements using the native rod disk membrane lipid environment show an appreciable increase in K_{eq} with increasing phosphorylation.

RDM vs Reconstituted Lipid Vesicles. RDM and PC vesicles differ in important ways that may help explain the opposite conclusions reached by these two studies. RDM are rich in loosely packed and highly mobile C22:6ω3 lipids that play an important role in allowing both rapid lateral diffusion and ready expansion of embedded proteins such as rhodopsin while POPC provides a less flexible environment. Metarhodopsin I undergoes a 70 cm^3/mol volume expansion upon metarhodopsin II formation and its formation

can be reversed by the application of external pressure (*30*). Membrane internal pressure can have important effects on MII yield and is strongly dependent on membrane lipid composition. Conversion of MI to MII can be blocked completely in micelles or vesicles composed of short-chain saturated lipids (*35*, *36*).

Lipid headgroup character also affects the MI−MII equilibrium through more than one mechanism. Smaller PS and PE headgroups of RDM dominate the cytoplasmic membrane surface while PC dominates the opposite leaflet. This distribution facilitates the MII yield by lowering the surface curvature free energy (*37*). In addition, PS has been shown to increase K_{eq} by augmenting the negative membrane surface potential (*38*). This results in a lower membrane surface pH, which stabilizes MII (*25*). Addition of negatively charged phosphates might similarly lower the local pH via its effect on surface charge and thus increase K_{eq} by a mechanism similar to that of PS.

Finally and perhaps most importantly, primary sequence and folding analysis of rhodopsin shows it to be strongly dipolar in character. In RDM, the cytoplasmic surface of rhodopsin (C-terminal face) bears a net charge of +4 while its extracellular or intradiscal (N-terminal) surface bears a nearly equal and opposite charge of −5 (*39*). While all rhodopsins have the same orientation in RDM, membrane proteins insert bidirectionally into lipid vesicle bilayers upon reconstitution. Bidirectional insertion would neutralize much of rhodopsin's native contribution to the system surface charge. A net surface charge near zero has been directly measured at the outer surface of PC vesicles using phosphonium spin probes (*39*). Our observation of MII enrichment with increasing phosphorylation in RDM may have been much smaller or nonexistent in lipid vesicles for one or more of the above reasons.

Physiological Implications. Rhodopsin phosphorylation alone can block signaling activity (*17*, *18*, *40*). An obvious candidate mechanism for this action is for phosphorylation to destabilize MII so that formation of one of the inactive conformations (MI or MIII) is favored. The conclusion of this paper, that phosphorylation instead increases the fraction of receptor in the activated state (MII) and its speed of formation, eliminates this possibility. However, this raises new questions about how or whether a negative regulatory function may be served by increasing the active form of the protein.

We speculate that MII stabilization by phosphorylation might accelerate the action of arrestin since arrestin selects only phosphorylated MII as its binding target (*41*). Initial phosphorylation may also facilitate multiple phosphorylation, if rhodopsin kinase prefers MII to other rhodopsin conformations (*42*, *43*), by augmenting the amount and rate of formation of MII from MI. This might contribute to the apparent cooperativity of rhodopsin phosphorylation (*16*, *44*, *45*).

In the absence of sufficient arrestin, such as would occur with very large bleaches, increased MII concentration that results from phosphorylation would favor decay of MII into the later-forming inactive conformer, metarhodopsin III. This would contribute to reduced receptor activity under conditions where the molar ratio of arrestin to rhodopsin is insufficient. Even without a direct effect of phosphorylation on rate or equilibrium constants for MIII formation, decay of light-activated rhodopsin (MI plus MII) into MIII must increase through mass action when the MII concentration increases due to phosphorylation.

Though it has been suggested that only two sites on rhodopsin (Ser-334 and Ser-338) are phosphorylated in vivo (*46*), the issue of phosphorylation number and sites is still unresolved (*47*); therefore, it is not clear that high phosphorylation levels are not physiologically relevant. We find significant changes in MII formation parameters at all phosphorylation stoichiometries.

This is the first study to report stabilization of an activated GPCR conformation by phosphorylation. It will be interesting to learn whether this is a general phenomenon applicable to other GPCR's and whether any of them might also show agonist-bound inactive states analogous to MI or MIII.

REFERENCES

1. Liebman, P. A., and Pugh, E. N., Jr. (1979) *Vis. Res. 19*, 375−380.
2. Liebman, P. A., and Pugh, E. N., Jr. (1980) *Nature 287*, 734−736.
3. Sibley, D. R., Strasser, R. H., Caron, M. G., and Lefkowitz, R. J. (1985) *J. Biol. Chem. 260*, 3883−3886.
4. Strasser, R. H., Sibley, D. R., and Lefkowitz, R. J. (1986) *Biochemistry 25*, 1371−1377.
5. Sitaramayya, A., and Liebman, P. A. (1983) *J. Biol. Chem. 258*, 1205−1209.
6. Benovic, J. L., Strasser, R. H., Caron, M. G., and Lefkowitz, R. J. (1986) *Proc. Natl. Acad. Sci. U.S.A. 83*, 2797−2801.
7. Palczewski, K. (1997) *Eur. J. Biochem. 248*, 261−269.
8. Surya, A., Foster, K. W., and Knox, B. E. (1995) *J. Biol. Chem. 270*, 5024−5031.
9. Jager, S., Palczewski, K., and Hofmann, K. P. (1996) *Biochemistry 35*, 2901−2908.
10. Emeis, D., Kuhn, H., Reichert, J., and Hofmann, K. P. (1982) *FEBS Lett. 143*, 29−34.
11. Bennett, N., Michel-Villaz, M., and Kuhn, H. (1982) *Eur. J. Biochem. 127*, 97−103.
12. Kibelbek, J., Mitchell, D. C., Beach, J. M., and Litman, B. J. (1991) *Biochemistry 30*, 6761−6768.
13. Kühn, H., and Dreyer, W. J. (1972) *FEBS Lett. 20*, 1−6.
14. Bownds, D., Dawes, J., Miller, J., and Stahlman, M. (1972) *Nature 237*, 125−127.
15. Frank, R. N., Cavanagh, H. D., and Kenyon, K. R. (1973) *J. Biol. Chem. 248*, 596−609.
16. Wilden, U., and Kuhn, H. (1982) *Biochemistry 21*, 3014−3022.
17. Sitaramayya, A. (1986) *Biochemistry 25*, 5460−5468.
18. Bennett, N., and Sitaramayya, A. (1988) *Biochemistry 27*, 1710−1715.
19. Liebman, P. A., Parker, K. R., and Dratz, E. A. (1987) *Annu. Rev. Physiol. 49*, 765−791.
20. Yee, R., and Liebman, P. A. (1978) *J. Biol. Chem. 253*, 8902−8909.
21. Knowles, A., and Dartnall, J. A. (1977) in *The Eye* (Davson H., Ed.) pp 53−101, Academic Press, New York.
22. Parkes, J. H., and Liebman, P. A. (1984) *Biochemistry 23*, 5054−5061.
23. Parkes, J. H., and Liebman, P. A. (1994) *Biophys. J. 66*, 80−88.
24. Emeis, D., and Hofmann, K. P. (1981) *FEBS Lett. 136*, 201−207.
25. Matthews, R. G., Hubbard, R., Brown, P. K., and Wald, G. (1963) *J. Gen. Physiol. 47*, 215−240.
26. Arnis, S., and Hofmann, K. P. (1993) *Proc. Natl. Acad. Sci. U.S.A. 90*, 7849−7853.
27. Thorgeirsson, T. E., Lewis, J. W., Wallace-Williams, S. E., and Kliger, D. S. (1993) *Biochemistry 32*, 13861−13872.
28. Liebman, P. A., and Sitaramayya, A. (1984) *Adv. Cyclic Nucleotide Protein Phosphorylation Res. 17*, 215−225.
29. Wilden, U., Hall, S. W., and Kuhn, H. (1986) *Proc. Natl. Acad. Sci. U.S.A. 83*, 1174−1178.

30. Lamola, A. A., Yamane, T., and Zipp, A. (1974) *Biochemistry 13*, 738−745.
31. Attwood, P. V., and Gutfreund, H. (1980) *FEBS Lett. 119*, 323−326.
32. Gibson, N. J., and Brown, M. F. (1993) *Biochemistry 32*, 2438−2454.
33. Brown, M. F. (1994) *Chem. Phys. Lipids 73*, 159−180.
34. Mitchell, D. C., Kibelbek, J., and Litman, B. J. (1992) *Biochemistry 31*, 8107−8111.
35. O'Brien, D. F., Costa, L. F., and Ott, R. A. (1977) *Biochemistry 16*, 1295−1303.
36. Baldwin, P. A., and Hubbell, W. L. (1985) *Biochemistry 24*, 2624−2632.
37. Wiedmann, T. S., Pates, R. D., Beach, J. M., Salmon, A., and Brown, M. F. (1988) *Biochemistry 27*, 6469−6474.
38. Gibson, N. J., and Brown, M. F. (1991) *Biochem. Biophys. Res. Commun. 176*, 915−921.
39. Tsui, F. C., Sundberg, S. A., and Hubbell, W. L. (1990) *Biophys. J. 57*, 85−97.
40. Palczewski, K., Rispoli, G., and Detwiler, P. B. (1992) *Neuron 8*, 117−126.
41. Schleicher, A., Kuhn, H., and Hofmann, K. P. (1989) *Biochemistry 28*, 1770−1775.
42. Yamamoto, K., and Shichi, H. (1983) *Biophys. Struct. Mech. 9*, 259−267.
43. Seckler, B., and Rando, R. R. (1989) *Biochem. J. 264*, 489−493.
44. Aton, B. R., Litman, B. J., and Jackson, M. L. (1984) *Biochemistry 23*, 1737−1741.
45. Adamus, G., Arendt, A., Hargrave, P. A., Heyduk, T., and Palczewski, K. (1993) *Arch. Biochem. Biophys. 304*, 443−447.
46. Ohguro, H., Van Hooser, J. P., Milam, A. H., and Palczewski, K. (1995) *J. Biol. Chem. 270*, 14259−14262.
47. Zhang, L., Sports, C. D., Osawa, S., and Weiss, E. R. (1997) *J. Biol. Chem. 272*, 14762−14768.

BI980933W